SOLAR PHYSICS FROM SPACELAB 2

K. Dere

JOURNAL DE PHYSIQUE
Colloque C1, Supplément au n°3, Tome 49, Mars 1988

SOLAR PHYSICS FROM SPACELAB 2

K.P. DERE

E.O. Hulburt Center for Space Research, Naval Research Laboratory, Washington, DC 20375, U.S.A.

Abstract - Four instruments were flown aboard the Spacelab 2 shuttle mission to perform systematic observations of the solar atmosphere at high resolution and to measure specific global properties of the sun. The Solar Optical Universal Polarimeter recorded series of white light images with which the evolution of the granulation and sunspot phenomena have been studied. The Coronal Helium Abundance Shuttle Experiment provided measurements of a number of EUV coronal lines, and, in particular, the intensities of He II λ304 and H I λ1216 from which the coronal helium abundance can be determined. The High Resolution Telescope and Spectrograph obtained stigmatic spectra in the 1200-1700 Å wavelength range, as well as broad band UV spectroheliograms, to provide diagnostic information on the solar chromosphere and transition zone. The Solar Ultraviolet Spectral Irradiance Monitor measured the total solar irrandiance at a resolution of 1.5 and 50 Å in the 1200 to 4000 Å wavelength range to an accuracy of 3%.

INTRODUCTION

The four solar experiments on the Spacelab 2 mission were mounted together on a single platform which was pointed at the sun by the Instrument Pointing System (IPS). An ambitious program of coordinated observations were planned to study the structure and dynamics of the solar atmosphere from the photosphere, through the chromosphere and transition zone and into the corona. In addition, the coronal helium abundance and the total solar untraviolet spectral irradiance were to be determined.

THE SOLAR OPTICAL UNIVERSAL POLARIMETER (SOUP)

SOUP (P.I., A. Title) was flown on the shuttle to get above the turbulent atmosphere that typically limits seeing to about an arc-second. Its purpose was to record sequences of high resolution images of the sun in integrated visible light and images of the photospheric magnetic and velocity fields. The magnetic field strength is measured by means of the Zeeman effect in lines of Fe I, although this part of the experiment was not successful. The high quality series of white light images have led to new results on the dynamics of the granulation. A typical white light image obtained by SOUP is shown in Fig. 1, where a sunspot, several pores and the ubiquitous granulation can be seen. Previous observations have shown that granules often come to an end as an "exploding granule." The Spacelab data indicates that essentially all granules are terminated by such explosions, whether in an individual granule or in a neighboring granule. The supergranular flow pattern is also detected by following the proper motions of individual granules in the Spacelab data.

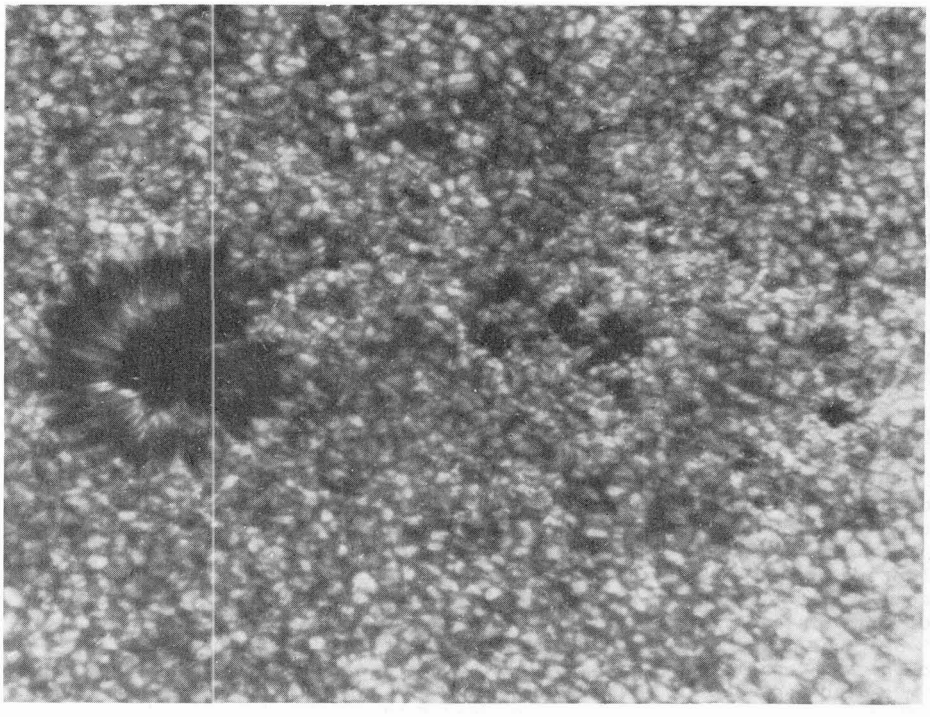

Fig. 1 - SOUP white-light image of a solar active region

THE CORONAL HELIUM ABUNDANCE SHUTTLE EXPERIMENT (CHASE)

CHASE (Co-P.I.'s J.L. Culhane and A. Gabriel) was designed to accurately determine the coronal helium abundance through the measurement of the coronal intensities of resonantly scattered H Lyα λ1216 and He II Lyα λ304 relative to their values on the solar disk. The instrument has the further capability to measure the intensities of a variety of useful EUV diagnostic lines. It uses a grazing incidence telescope which focuses an image of the sun onto the slit of the grazing incidence spectrograph. The radiation is detected by 11 channel electron multipliers together with a channel multiplier array plate, so that a complement of 12 primary spectral lines in the 150-1335 Å wavelength range can be observed as well as a variety of nearby secondary lines. The telescope mirror can be translated to perform spatial scans and the spectrograph slit can also be moved to perform raster scans of a small solar area. Spectral scans are performed by rocking the grating.

The basic set of measurements consisted of disk and coronal intensities of the hydrogen and helium lines. The coronal helium abundance relative to hydrogen is then calculated from the following formula:

$$N_{He}/N_H = 16\ A(T)\ R_p(T)\ (I_{304}/I_{1216})/(F_{1216}/F_{304})$$

where I is the coronal intensity and F is the disk brightness. A(T) is the ratio of the H I and He II relative ion abundances and $R_p(T)$ is the ratio of the coronal scattering rates. The combined temperature dependence of A and R_p is $T^{1/4}$ so that the method is relatively insensitive to the coronal temperature. Since the value of the helium abundance depends only on the ratio of disk to coronal intensities,

the ability to make the abundance determination is greatly improved because the instrumental sensitivity is not involved. In Fig. 2, measurements of the hydrogen

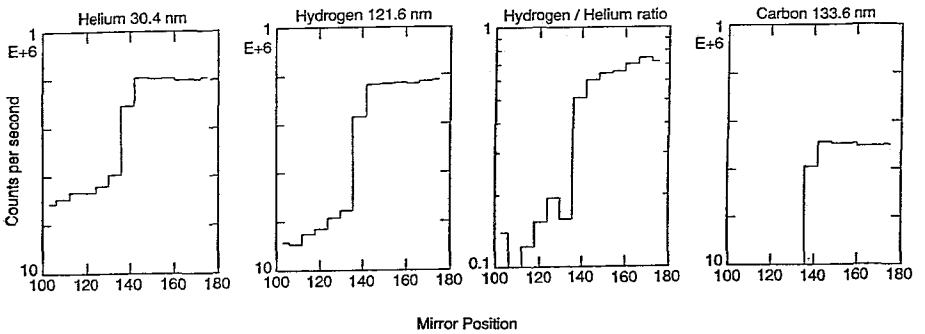

Fig. 2 - CHASE intensities measured at the limb

and helium intensities, obtained in spatial scans outward across the solar limb, are shown. Also shown is the intensity ratio of the hydrogen and helium lines and the intensity of C II λ1335 which clearly shows the position of the solar limb.

High quality data on the hydrogen and helium intensities on and off the disk were obtained but the essential secondary data for the in-flight measurement of the telescope scattering was largely lost as a result of the inadequate pointing performance of the IPS. The scattering function has not been obtained from the data with sufficient accuracy. Preliminary values of the helium to hydrogen abundance are consistent, within large error bars, with the currently accepted value of 0.1 [1]. Measurements of the telescope scatter is presently being made in the laboratory and should permit a much better abundance determination.

THE HIGH RESOLUTION TELESCOPE AND SPECTROGRAPH (HRTS)

HRTS (P.I. G. Brueckner) uses a 30 cm Gregorian telescope to focus an image of the sun onto the slit jaws of the UV spectrograph with 1 arc-second resolution. A broadband spectroheliograph views the spectrograph slit jaws to produce images of the integrated solar spectrum in a 100Å band centered on 1550Å. The main spectral components in the bandpass are the temperature minimum continuum, chromospheric lines and the C IV transition zone lines which dominate the spectrum above the limb. An observing sequence was executed to study the structure and evolution of high altitude transition zone structures over a 27 minute time period. A subset of these images is shown in Fig. 3 where the most dramatic feature is the birth of 2 large spicules and the growth of another. The observations were taken near the boundary of a polar coronal hole which, from Skylab observations [2], are known to produce macrospicules whose range of observed properties are similar to those observed in these large spicules, although the widths of the large spicules in Fig. 3 are at the extreme lower end of the range determined from the Skylab data. Their evolution can be interpreted either as the result of an upflow of C IV emitting material or by the uniform heating or cooling of a pre-existing structure.

The prime focal plane instrument is the tandem-Wadsworth UV spectrograph which operates in the 1200-1700 Å wavelength range. Stigmatic photographic spectra along a 900" (1 solar radius) long by 0.5" wide slit were recorded with typical exposure times of 2 to 20 s. By sequentially rastering the slit in 1 to 3" increments, line profiles in an extended solar area are obtained.

One of the more striking events observed in previous rocket flights of the HRTS were the coronal bullets or jets. These are 10" wide ejections of material that are accelerated at 5 km s^{-2} to velocities of 500 km s^{-1}. The global birthrate for these highly energetic events, extrapolated from short duration observations of a extremely small solar area, indicated a potentially significance role in the transport of matter and energy in the solar atmosphere. One of the goals of the Spacelab 2 mission was to observe a large fraction of the solar disk in order to determine their significance on a sound statistical basis. In the end, no examples of these extremely high velocity events were found although a large number of lower velocity (100 km s^{-1}) explosive events were detected and have been studied. These

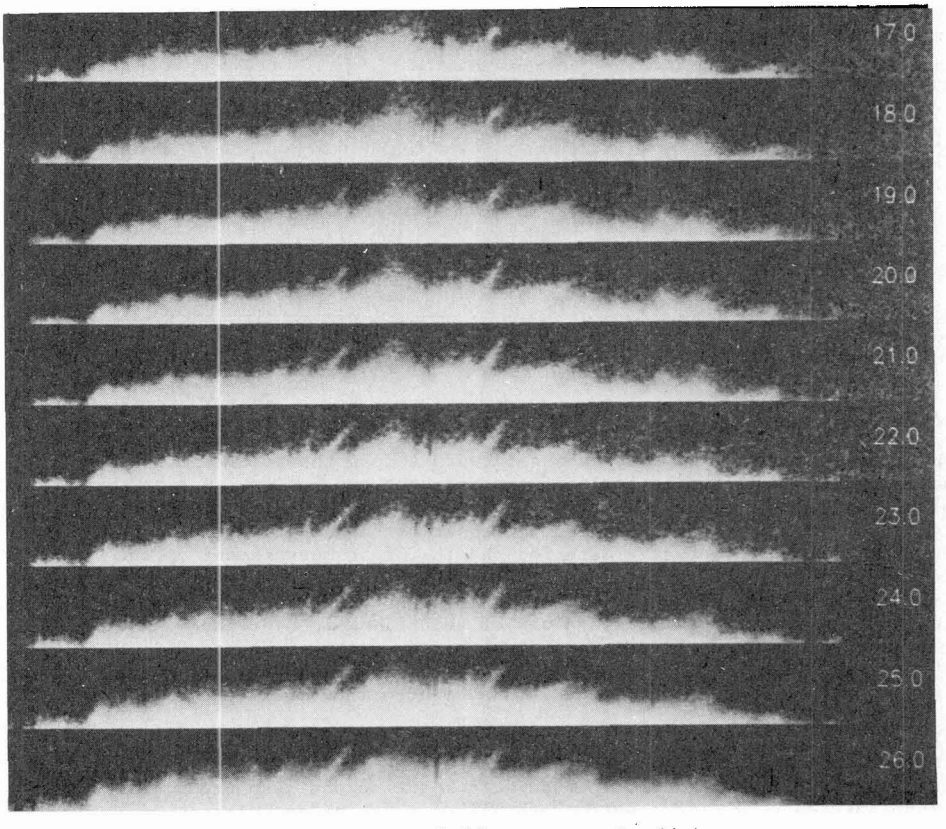

Fig. 3 - HRTS UV spectroheliograms at the limb

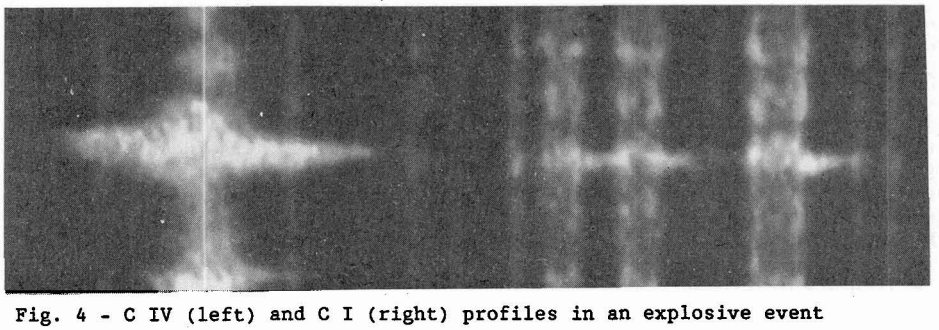

Fig. 4 - C IV (left) and C I (right) profiles in an explosive event

are a category of event that show strong Doppler shifts of 100 km s^{-1} to the blue and/or to the red in a compact (2") volume. In Fig. 4, C IV (left) and C I (right) spectra of an extraordinary explosive event near the solar limb is shown. This event is somewhat larger than the typical explosive event and the red wing of C IV shows velocities up to about 200 km s^{-1}. What makes this event extraordinary is the strong response in the chromospheric lines of C I which show red shifts of up to 100 km s^{-1}. There are only two such events among the hundreds observed during Spacelab 2 which show any signature of the explosive events in chromospheric lines. This would imply that explosive events occur at height, well above the chromosphere. Fig. 5 shows more examples of explosive events, again seen in C IV

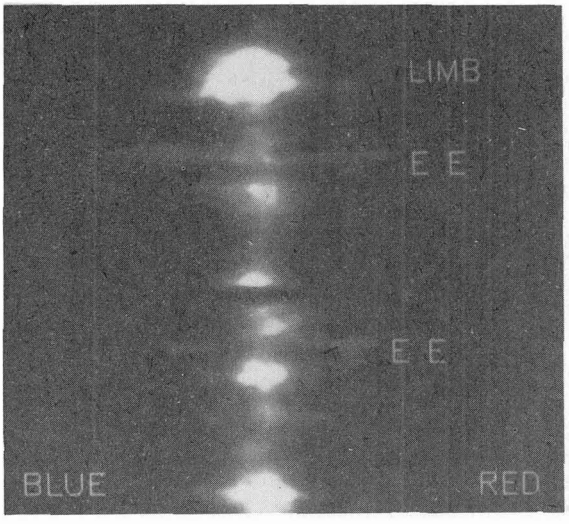

Fig. 5 - Explosive events in C IV

near the limb. The upper event (labelled 'EE') reveals a shallow 'V' pattern in the spectral pattern and the lower one shows a complete spatial discontinuity between the red and blue wings. These two events demonstrate that the explosive events have considerable spatial structure at arc-second resoluton. Many profiles of explosive events show a continuous distribution of velocities from the extreme blue to the extreme red wing. This brings up the question of the relative importance of turbulent and directed flows. In the upper profile with the 'V' shape, the turbulent velocities are much less than the directed flow velocities. The lower profile demonstrates that in many cases this can be attributed to the inability to resolve close-spaced but distint directed flows, although turbulent velocities may still be involved in this example. The data indicate the presence of strong directed flows in explosive events as well a possibly strong role for turbulent velocities in some events.

The analysis of a large number of explosive events observed during Spacelab 2 is contributing to our understanding of their physical properties on a statistical basis. Distributions of several measured physical parameters are shown in Fig. 6.

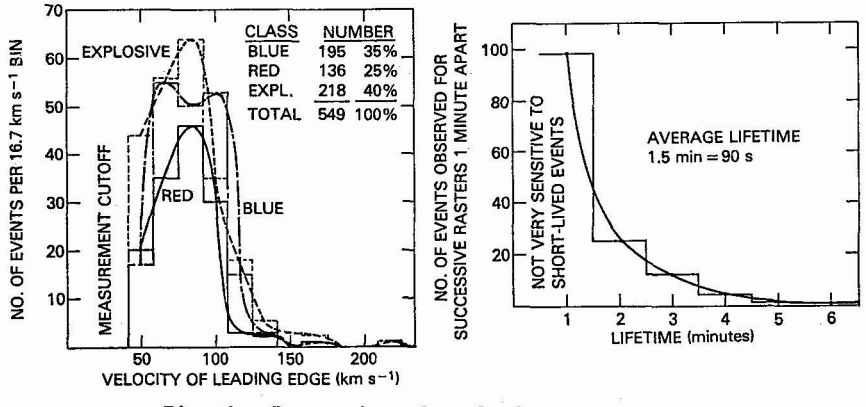

Fig. 6 - Properties of explosive events

The velocity distribution peaks near 80 km s^{-1} which is roughly the Alfven speed

for a magnetized plasma with an equipartition of thermal, turbulent and magnetic pressures. The sizes of the events are near 2" and they have lifetimes of 60 s or less. Estimates of the total global transport of energy in these events is about a factor of 10 or more below the energy required to sustain coronal energy losses. The actual numbers are strongly dependent on the fraction of the observed volume that is actually filled by C IV emitting material. For these events, the fill factor is perhaps well below unity.

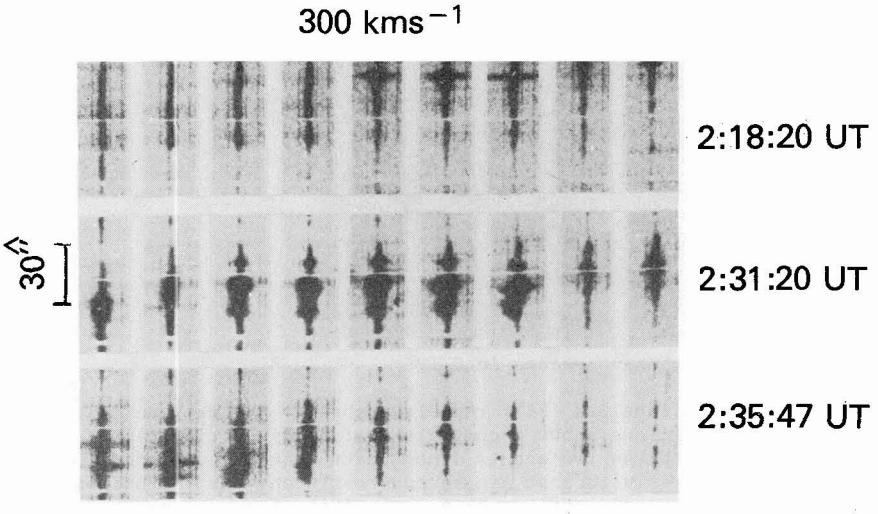

Fig. 7 - Turbulent C IV profiles associated with an EFR

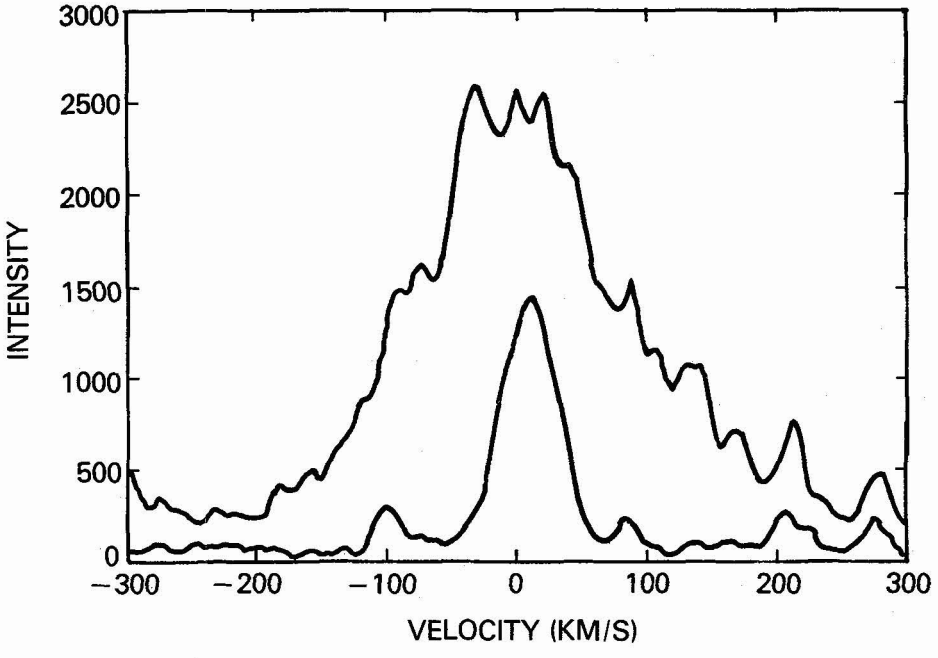

Fig. 8 - C IV profile at maximum phase

A possible scenario for producing the explosive events is the eruption of small

dipoles of magnetic flux through the solar atmosphere. It has not been possible to establish this link observationally because of a general lack of photospheric magnetograms obtained simultaneously with the HRTS spectra. In one exceptional case, it is been possible to show that high velocity C IV profiles are directly associated with emerging magnetic flux. Fig. 7 shows the widest, most "turbulent" profiles observed in all of the HRTS data. The spectra were obtained during three raster sequences of exposures. The region of high "turbulence" extends about 30" along the slit. While some of the profiles are roughly symmetric and may be the result of turbulent flows, there are also asymmmetric profiles indicating directed mass flows. The widest profile at maximum phase is plotted in Fig. 8 where velocities of up to 300 km s^{-1} are present in the red wing. For comparison, a narrower profile obtained earlier in this region is plotted. The Hα image obtained by the Hida Observatory at 7:06 UT, 5 hours later shows the classical structure of an emerging flux region in the area where the turbulent profiles are seen. Because of the emerging flux, the magnetic field geometry is clearly changing rapidly, resulting in increased magnetic shear which probably leads to reconnection from which the turbulent velocities might result.

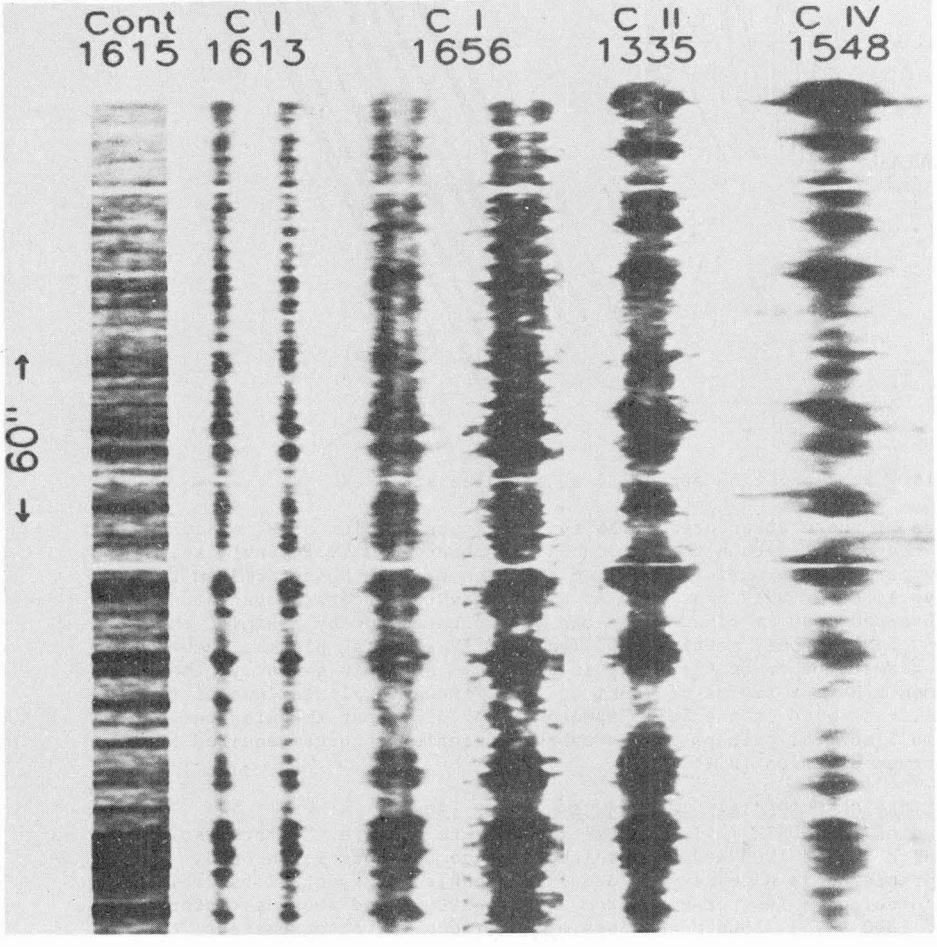

Fig. 9 - HRTS spectra in the quiet sun

The wavelength region in which the HRTS operates contains numberous strong spectral lines that provide valuable diagnostic information on the structure and dynamics of the solar chromosphere and transition zone. A selection of profiles

produced in the quiet sun are shown in Fig. 9. These spectra were obtained with the HRTS slit along a solar radius, with one end at the limb, at the top of the figure. From the left is the continuum produced in the temperature minimum region, next, the chromospheric intercombination line of C I λ1613 from consecutive 30 s and 10 s exposures, the self-reversed resonance line of C I λ1656 from consecutive 10 s and 3 s exposures, the resonance line of C II λ1335 from a 3 s exposure and C IV profiles from the same 3 s exposure. The continuum, the C I profiles and the C IV profiles all show that that most of the intensity is produced in small discrete structures along the slit. In the continuum, these can be identified as the footpoints of spicules, the extensions of which are seen in chromospheric lines of C I and then at higher altitudes and temperatures in C IV. Fig. 10 shows a

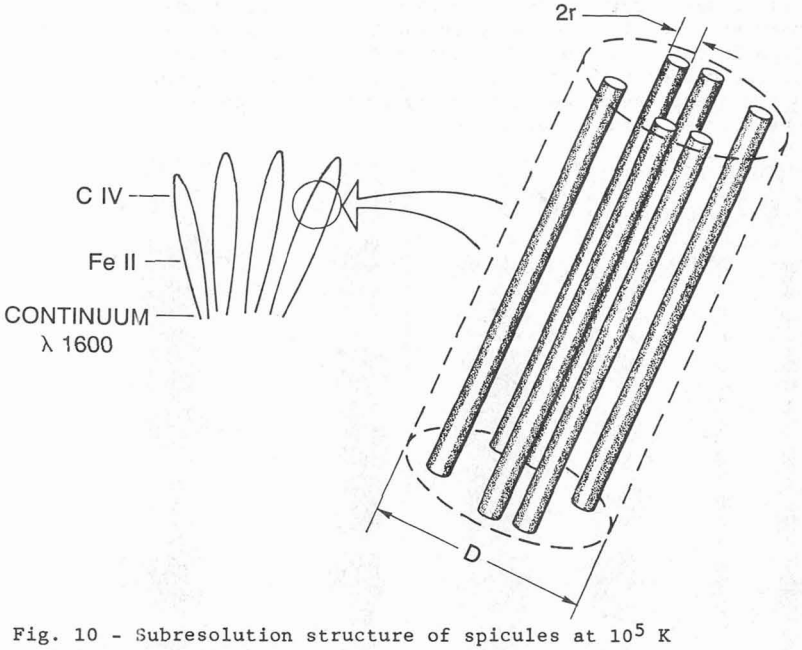

Fig. 10 - Subresolution structure of spicules at 10^5 K

schematic picture of these structures. The typical cross section of UV spicules is about 2000 km. The path length h that produces the observed C IV intensities, calculated from the emission measure $N_e^2 h$ and electron density N_e determined from density sensitive lines of O IV near 1400 Å, is roughly two orders of magnitude less than the observed 2000 km size. This can be accounted for by assuming that the observed structure is only partially filled by C IV emitting plasma, such as in the filamentary geometry show on the right in Fig. 10. For this geometry, the individual filaments have a radius of 70 km or less. Recent calculations of the dissipation of Alfven waves in the solar atmosphere predict that the dissipation must occur on small scales, perhaps in the subresolution structures required to explain the observed emission [3,4].

THE SOLAR ULTRAVIOLET SPECTRAL IRRADIANCE MONITOR (SUSIM)

The objective of the SUSIM (P.I. G. Brueckner) is to measure the total solar irradiance at earth in the 1200-4000 Å wavelength range at a precision of 5%. This quest for high precision is necessary in order to track solar spectral variability which is on the order of a few per-cent from 2000 to 3000 Å and about a factor of 2 between 1000 and 1600 Å [5]. SUSIM consists of two redundant spectrometers, seven detectors, each of which can be moved behind the exit slit of either spectrometer, and an inflight D_2 calibration source. Spectra are taken at either a 1.5 or 50 Å resolution. One spectrometer is used to determine the stability of the instrument and the second spectrometer to make the actual solar observations. Degradation in

instrumental sensitivity is a problem endemic to all solar UV instruments and was dramatically demonstrated by the HRTS which lost sensitivity at H Lyα λ1216 by two orders of magnitude or more. The primary calibration is carried out both before and after the flight at the National Bureau of Standards (NBS) synchrotron which has a reported absolute photometric accuracy of 0.7%. The opportunity to make a postflight calibration is one of the chief advantages of this program. The D_2 lamp is used to track changes in instrument sensitivity between NBS calibrations both during storage on the ground and during solar operations in flight. During the two year period of storage and solar operations between NBS synchrotron calibrations, the sensitivity of the solar spectrometer showed a degradation of 10% at 4000 Å and 38% at 1250 Å. Because the degradation is monitored by the D_2 calibrations, a high accuracy is maintained. The estimated RMS error (1 σ) in the final observed spectrum is 4% throughout the entire wavelength range.

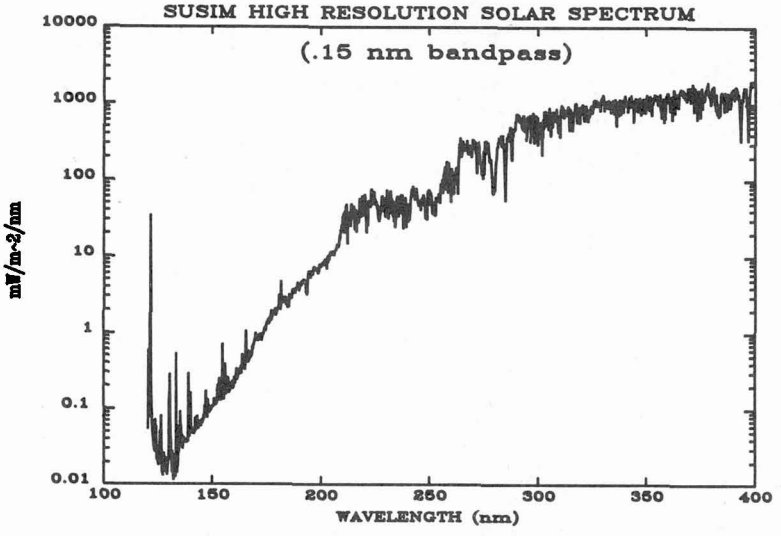

Fig. 11 - SUSIM high resolution solar spectrum

The high resolution SUSIM spectrum is shown in Fig. 11. The low resolution spectrum has been compared with the results from the Spacelab 1 measurements in the 2000-3500 Å wavelength range and differences of only 0.3%, on average, and 3% at maximum are found [6]. The high resolution spectrum has been compared with the measurements of Samain [7] and Moe [8]. The values of Samain agree with the SUSIM values above 1800 Å but below about 1700 Å where the values of Moe and Samain are in agreement, the SUSIM values are about a factor of 2 higher. These differences remain to be sorted out.

References

[1] J.P. Meyer 1985, Ap. J. Suppl. 57, 173.
[2] J.D. Bohlin, S.N. Vogel, J.D. Purcell, N.R. Sheeley, R. Tousey, and M.E. VanHoosier 1975, Ap. J. Letters 197, L133.
[3] J. Davila 1987, Ap. J. 317, 514.
[4] G. Einaudi and Y. Mok 1987, Ap. J. 319, 520.
[5] J. Lean 1987, J. Geophys. Res. 92, D1, 839.
[6] D. Labs, H. Neckel, P.C. Simon and G. Thullier 1987, Solar Phys. 107, 203.
[7] D. Samain 1979, Astron. Astrophys. 74, 225.
[8] O. Kjeldseth Moe, M.E. VanHoosier, J.-D.F. Bartoe, and G.E. Brueckner 1796, Naval Research Laboratory Report 8056.